

# Weierstraß-Institut für Angewandte Analysis und Stochastik

im Forschungsverbund Berlin e.V.

Preprint

ISSN 0946 – 8633

## Phase transition and hysteresis in a rechargeable lithium battery

Wolfgang Dreyer<sup>1</sup>, Miran Gaberšček<sup>2</sup> and Janko Jamnik<sup>2</sup>

submitted: 20th December 2007

<sup>1</sup> Weierstrass-Institute  
for Applied Analysis  
and Stochastics  
Mohrenstr. 39  
10117 Berlin  
Germany  
E-Mail: dreyer@wias-berlin.de

<sup>2</sup> Kemijski Inštitut Ljubljana Slovenija  
L10 Laboratory for Materials Electrochemistry  
SI-1001 Ljubljana  
Hajdrihova 19  
Slovenija  
E-Mail: miran.gabrscek@ki.si  
janko.jamnik@ki.si

No. 1284

Berlin 2007



---

2000 *Mathematics Subject Classification.* 74N20, 74A15, 74N05, 74B99.

*Key words and phrases.* lithium-ion-battery, FePO<sub>4</sub>, thermodynamics, phase transitions, hysteresis, chemical potentials, surface stress, deviatoric stress, elasticity.

Edited by  
Weierstraß-Institut für Angewandte Analysis und Stochastik (WIAS)  
Mohrenstraße 39  
10117 Berlin  
Germany

Fax: + 49 30 2044975  
E-Mail: [preprint@wias-berlin.de](mailto:preprint@wias-berlin.de)  
World Wide Web: <http://www.wias-berlin.de/>

## Abstract

We develop a model which describes the evolution of a phase transition that occurs in some part of a rechargeable lithium battery during the process of charging/discharging. The model is capable to simulate hysteretic behavior of the voltage - charge characteristics.

During discharging of the battery, the interstitial lattice sites of a small crystalline host system are filled up with lithium atoms and these are released again during charging. We show within the context of a sharp interface model that two mechanical phenomena go along with a phase transition that appears in the host system during supply and removal of lithium. At first the lithium atoms need more space than it is available by the interstitial lattice sites, which leads to a maximal relative change of the crystal volume of about 6%. Furthermore there is an interface between two adjacent phases that has very large curvature of the order of magnitude 100 m, which evoke here a discontinuity of the normal component of the stress. In order to simulate the dynamics of the phase transitions and in particular the observed hysteresis we establish a new initial and boundary value problem for a nonlinear PDE system that can be reduced in some limiting case to an ODE system.

## 1 Introduction

The arrangement shown in Figure 1 roughly indicates the processes in a lithium battery during discharging and charging. During discharging electrons leave the anode to travel through an outer circuit. The anode is here assumed to be a metallic lithium electrode. The remaining positive lithium ions leave the anode and move through an electrolyte towards the cathode, which is the central object of the current modelling. It consists of a carbon coated single crystal  $\text{FePO}_4$  with the shape of a small sphere of about 50 nm diameter. The  $\text{FePO}_4$  lattice offers interstitial lattice sites that serve to store lithium atoms. When the battery is fully charged, all interstitial lattice sites are empty. During discharging the arriving lithium ions combine at the carbon coated surface of the  $\text{FePO}_4$  ball with the inflowing electrons and hereafter they occupy the interstitial lattice sites. After complete discharging a maximal number of sites of the interstitial lattice is occupied by a lithium atom. During recharging of the battery the reverse process takes place.

The objective of the current study is the modelling of the loading/unloading processes of the  $\text{FePO}_4$  lattice with Lithium atoms. The model describes diffusion with mechanical coupling within an open system. It relies on various experimental observations and assumptions:

1. The voltage - charge plot, see Figure 2 exhibits a hysteretic behavior. The characteristics of voltage against the total charge of the battery during charging, red arrows, is different from discharging, blue arrows.

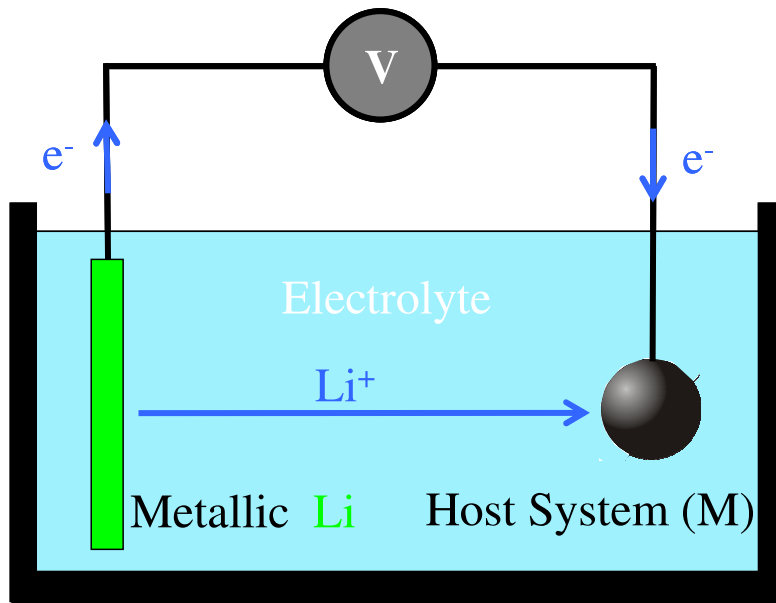


Figure 1: Basic constituents of a rechargeable lithium battery

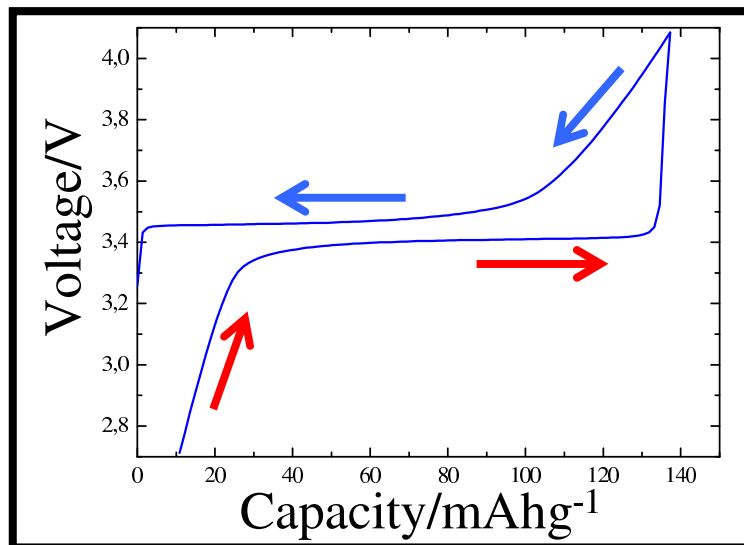


Figure 2: Typical charge and discharge curve for a LiFePO<sub>4</sub> cathode. The voltage is plotted as a function of the total charge per mass. The charging (red arrows) and discharging (blue arrows) were performed under constant current regime. The electrode was prepared as described elsewhere [6].

2. The lithium atoms need more space as it is offered by the interstitial lattice sites. In case of a fixed external pressure, this leads to a change of the volume of the  $\text{FePO}_4$  ball up to 6% for the fully occupied interstitial lattice.
3. There is a compact region of total lithium fraction where the distribution of the lithium atoms within the  $\text{FePO}_4$  ball decomposes into two phases with different local lithium fractions across the interface between the adjacent phases. Currently we assume that there is a single interface with the shape of a sphere. Thus in the 2-phase region we currently deal with an inner core and an outer shell. Furthermore we assume that the interface originates at the outer surface during loading as well as during unloading.
4. At the interface of the two phases we take surface tension into account, which is of enormous importance due to the small interfacial radius.

Further assumptions will be given later on. Here we remark that the volume change of the  $\text{FePO}_4$  ball and the incorporation of surface tension at the interface lead within the model to a hysteretic behavior of the loading/unloading process.

Finally we mention a recent study, see [11], by Wagemaker, Borghols and Mulder. The authors observe a strong dependence between the maximal possible Li content and the size of the host system, and they conjecture likewise mechanical effects as the origin for this phenomenon. In fact, it is a typical feature of the mechanical boundary value problem, that the size of the considered system is of large influence.

We have organized the paper as follows:

In Chapter 2 we describe the constitution of the host system. The thermodynamic model is developed in Chapter 3 and extended in the appendix. This model relies on local conservation laws in the bulk phases, on jump conditions, i.e. Stefan conditions, across the interface and in particular on so called kinetic relations, which determine the interfacial motion and the evolution of the atomic lithium fractions on both sides of the interface. We end up with a system of nonlinear diffusion equations with mechanical coupling.

Chapter 4 considers the limiting case of infinite bulk mobility, whereby we may reduce the PDE system into an ODE system for the atomic Li fraction, the interfacial radius and the external radius of the  $\text{FePO}_4$  ball as functions of time.

Various simulations are the content of Chapter 5. We illustrate the influence of the mechanical phenomena on the relevant chemical potentials. We determine the possible equilibria and we extract from these data the hysteric behavior of the loading/unloading processes. Finally we simulate the evolution of the host system for various initial data.

## 2 Constitution of the host system

The mechanical constitution of the host system from Figure 1 is described in detail by T. Maxisch and G. Ceder in [9]. It is composed of a deformable crystal lattice of the substance  $\text{FePO}_4$ . The undeformed crystal has orthorhombic olivine symmetry. Furthermore there is a sublattice whose lattice sites may be empty or occupied by Li atoms. These can be supplied or removed through the external boundary, and this process is called *lithiation*. To each unit of  $\text{FePO}_4$  there corresponds one single site in the sublattice. The occupation of the sublattice with Li atoms does not change the orthorhombic olivine symmetry. However, the elastic stiffness coefficients and the crystal volume change if the number of Li atoms is changed.

At room temperature there exists a region of total Li concentration where the distribution of Li atoms on the sublattice sites is realized by two coexisting phases that differ by high and small Li concentrations. Theoretical studies on the evolution of Li atoms in the host system by Han et.al [8], Srinivasan and Newman [10] and the current study rely on this phenomenon, which is experimentally investigated by Yamada et.al. [12].

Based on previous studies by Srinivasan and Newman [10] and Han et.al [8], we currently also assume that the two phases exhibit a simple morphology: They appear as an inner spherical core and an outer shell with a moving interface. However, it is important to note that in 2007 this assumed symmetry is criticized by Allen, Jow and Wolfenstine [1]. Due to some experimental hints these authors prefer a plane interface that may move in some preferred direction of the matrix lattice. For this reason we have formulated the current model in a form so that this case is included, see in particular the appendix. In other words, only the current numerical exploitation of the model relies on the spherical core assumption, so that we may follow Allen et al.'s proposal in a further study.

## 3 Thermodynamic description of the host system

### 3.1 Conservation laws of particle numbers

We consider the host system as a body  $\Omega$  that may be represented by a single phase or by two coexisting phases, so that  $\Omega = \Omega_- \cup \Omega_+$  as it is indicated in Figure 3.  $\Omega_-$  and  $\Omega_+$  denote the inner core with radius  $r_1$  respectively the outer shell with radius  $r_0$ . At any time  $t \geq 0$ , the thermodynamic state of the body  $\Omega$  is described by a certain number of variables, which may be functions of space  $x = (x^i)_{i=1,2,3} = (x^1, x^2, x^3) \in \Omega$ . The host system consists of three constituents: There are  $\text{FePO}_4$  units (M) generating the deformable lattice, which we shall call the matrix lattice. The matrix lattice has orthorhombic symmetry in the undeformed state. Furthermore there is an interstitial sublattice, whose constituents are Li - atoms (Li) and vacancies (V). The number densities of the constituents are denoted

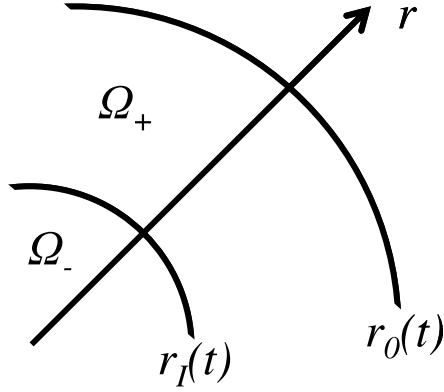


Figure 3: The 2-phase morphology of the host system

by  $n_M$ ,  $n_{Li}$  and  $n_V$ .

Among the objectives of this study is the determination of the functions

$$n_M(t, x), \quad n_{Li}(t, x), \quad n_V(t, x) \quad \text{and} \quad r_I(t), \quad r_0(t). \quad (1)$$

We assume that there is no diffusion on the matrix lattice, which is fully occupied by the  $\text{FePO}_4$  units, so that  $n_M(t, x)$  changes exclusively due to the deformation of the lattice. On the sublattice we have diffusion, which, however, is restricted by the side condition that matrix lattice and sublattice have equal number of lattice sites, thus we have

$$n_M(t, x) = n_{Li}(t, x) + n_V(t, x). \quad (2)$$

Next we introduce the velocities  $v = (v^i)_{i=1,2,3} = (v^1, v^2, v^3)$  of the constituents by the functions

$$v_M(t, x), \quad v_{Li}(t, x), \quad v_V(t, x) \quad (3)$$

According to the constraint (2) we relate the velocity of the matrix to the other velocities by

$$n_M v_M(t, x) = n_{Li} v_{Li}(t, x) + n_V v_V(t, x). \quad (4)$$

The constraint (4) is motivated by the conservation laws for the particle numbers, which read in regular points of  $\Omega$

$$\frac{\partial n_M}{\partial t} + \text{div}(n_M v_M) = 0, \quad \frac{\partial n_{Li}}{\partial t} + \text{div}(n_{Li} v_{Li}) = 0, \quad \frac{\partial n_V}{\partial t} + \text{div}(n_V v_V) = 0. \quad (5)$$

Due to (2) and (4) there are only two independent conservation laws, and we prefer to deal with  $(5)_1$  and  $(5)_2$  in the sequel.

If the state of the host system is in the 2-phase region, singular points will appear at the interface  $I$  between the adjacent phases. At  $I$  the conservation laws of particle

numbers assume the form

$$-w^\nu [[n_M]] + [[n_M v_M^\nu]] = 0, \quad -w^\nu [[n_{Li}]] + [[n_{Li} v_{Li}^\nu]] = 0, \quad -w^\nu [[n_V]] + [[n_V v_V^\nu]] = 0. \quad (6)$$

Herein  $w^\nu$  denotes the normal speed of the interface and  $\nu$  is the normal vector, which points into the + region. The double bracket gives the difference of a quantity that suffers a discontinuity at the interface:  $[[\psi]] \equiv \psi_+ - \psi_-$ .

We conclude that the atomic fluxes

$$\dot{\mathcal{N}}_M \equiv -n_M(v_M^\nu - w^\nu), \quad \dot{\mathcal{N}}_{Li} \equiv -n_{Li}(v_{Li}^\nu - w^\nu) \quad \text{and} \quad \dot{\mathcal{N}}_V \equiv -n_V(v_V^\nu - w^\nu) \quad (7)$$

are continuous across the interface, i.e.

$$\dot{\mathcal{N}}_M^+ = \dot{\mathcal{N}}_M^-, \quad \dot{\mathcal{N}}_{Li}^+ = \dot{\mathcal{N}}_{Li}^-, \quad \text{and} \quad \dot{\mathcal{N}}_V^+ = \dot{\mathcal{N}}_V^-. \quad (8)$$

In the considered case of spherical morphology, the interface is completely described by its time dependent radius  $r_I(t)$ . In this case we have in polar coordinates  $\nu = (1, 0, 0)$  and  $w^\nu = \dot{r}_I(t)$ . Likewise in the bulk, we take (8)<sub>1</sub> and (8)<sub>2</sub> as the two independent conservation laws for  $x \in I$ .

The quantities that appear in the conservation laws of particle numbers can be combined to define further quantities that are needed for the description of the thermodynamic state of the host system. Among these are the mass density  $\rho$  and the barycentric velocity  $v$ , which are defined by

$$\rho \equiv m_{Li}n_{Li} + m_M n_M \quad \text{and} \quad \rho v \equiv m_{Li}n_{Li}v_{Li} + m_M n_M v_M, \quad (9)$$

where  $m_M$  and  $m_{Li}$  denote the atomic masses of  $\text{FePO}_4$  and Li. Note that the vacancies do not contribute to mass density and barycentric velocity.

A linear combination of the conservations laws for particle numbers imply the conservation laws for the total mass, viz.

$$\frac{\partial \rho}{\partial t} + \text{div}(\rho v) = 0 \quad \text{for} \quad x \in \Omega_{+/-} \quad \text{and} \quad -w^\nu [[\rho]] + [[\rho v^\nu]] = 0 \quad \text{for} \quad x \in I. \quad (10)$$

Next we introduce the atomic fraction of Li,  $y$ , and the diffusion fluxes with respect to the velocity  $v_M$  of the crystal lattice,  $j_{Li} = (j_{Li}^i)_{i=1,2,3}$  and  $j_V = (j_V^i)_{i=1,2,3}$ :

$$y \equiv \frac{n_{Li}}{n_M}, \quad j_{Li} \equiv n_{Li}(v_{Li} - v_M), \quad j_V \equiv n_V(v_V - v_M). \quad (11)$$

Diffusion fluxes with respect to the barycentric velocity  $v$  are also important,  $f_{Li} = (f_{Li}^i)_{i=1,2,3}$ ,  $f_V = (f_V^i)_{i=1,2,3}$  and  $f_M = (f_M^i)_{i=1,2,3}$ :

$$f_{Li} \equiv n_{Li}(v_{Li} - v), \quad f_V \equiv n_V(v_V - v) \quad \text{and} \quad f_M \equiv n_M(v_V - v). \quad (12)$$

Finally we list several identities between the various diffusion fluxes. They read

$$j_{Li} + j_V = 0, \quad m_{Li}f_{Li} + m_M f_M = 0, \quad f_{Li} = j_{Li} + y f_M, \quad f_V = j_V + (1 - y) f_M, \quad (13)$$

and at the interface we have

$$m_{Li}\dot{\mathcal{N}}_{Li} + m_M \dot{\mathcal{N}}_M = -\rho(v^\nu - w^\nu). \quad (14)$$



### 3.2 Conservation law of momentum

The conservation law of momentum determines the motion of the matrix lattice, i.e. the displacement  $u = (u^i)_{i=1,2,3} = (u^1, u^2, u^3)$ . If we ignore elastic waves in the matrix lattice, this conservation law reduces to a quasi-static force balance, which reads in regular points in  $\Omega$

$$\operatorname{div} \sigma = 0. \quad (15)$$

The newly introduced quantity  $\sigma = (\sigma^{ij})_{i,j=1,2,3}$  is the Cauchy stress tensor with  $\sigma^{ij} = \sigma^{ji}$ . The detailed description of motion, strain and stresses will be given in the Appendix, because here we apply a simplified mechanical model that ignores (i) the orthorhombic symmetry and (ii) the deviatoric stresses so that the stress tensor reduces to a pressure  $p$ :  $\sigma^{ij} = -p\delta^{ij}$ .

The quasi-static momentum balance at the interface  $I$  is given by

$$[[\sigma^{ij}]]\nu^j = -2\gamma k_M \nu^i, \quad \text{respectively for the special case at hand} \quad [[p]] = -\frac{2\gamma}{r_I}. \quad (16)$$

$\gamma > 0$  is the surface tension and  $k_M$  denotes the mean curvature, which reads in polar coordinates for a sphere:  $k_M = -1/r_I$ .

### 3.3 Constitutive Model, Part 1: Some pieces of the second law of thermodynamics

In this and the following sections we rely on the recent study by Dreyer et.al. [2] to show that the knowledge of the free energy is sufficient in order to give all constitutive quantities as functions of the variables. Here we start with the assumption that the specific free energy,  $\psi$ , is given by the general representations

$$\psi = \hat{\psi}(T, n_{\text{Li}}, n_{\text{V}}) = \tilde{\psi}(T, y, \rho). \quad (17)$$

The both functions  $\hat{\psi}$  and  $\tilde{\psi}$  are related to each other in a simple manner by means of the transformation

$$y = \frac{n_{\text{Li}}}{n_{\text{Li}} + n_{\text{V}}} \quad \text{and} \quad \rho = (n_{\text{Li}} + n_{\text{V}})m(y) \quad \text{with} \quad m(y) \equiv m_{\text{M}} + m_{\text{Li}}y. \quad (18)$$

In the following, the function  $\hat{\psi}$  will be used to calculate the chemical potentials  $\mu_{\text{Li}}$  and  $\mu_{\text{V}}$  whereas  $\tilde{\psi}$  gives the pressure  $p$ . According to the 2<sup>nd</sup> law of thermodynamics we have, see [2] for details,

$$\mu_{\text{Li}} = \frac{\partial \rho \hat{\psi}}{\partial n_{\text{Li}}}, \quad \mu_{\text{V}} = \frac{\partial \rho \hat{\psi}}{\partial n_{\text{V}}}, \quad p = \rho^2 \frac{\partial \tilde{\psi}}{\partial \rho}, \quad \rho \psi + p = \mu_{\text{Li}} n_{\text{Li}} + \mu_{\text{V}} n_{\text{V}}. \quad (19)$$

The equations (19)<sub>1</sub> to (19)<sub>3</sub> give some parts of the Gibbs equation and (19)<sub>4</sub> is called Gibbs-Duhem equation. The explicit form of the functions  $\hat{\psi}$  and  $\tilde{\psi}$  will be given and exploited in the next Section.

A further content of the 2<sup>nd</sup> law of thermodynamics is the entropy inequality, which identifies on its left hand side the entropy production in the two bulk phases. It reads

$$-f_{\text{Li}}\nabla\mu_{\text{Li}} - f_{\text{V}}\nabla\mu_{\text{V}} = -f_{\text{Li}}\nabla\left(\mu_{\text{Li}} - \frac{m_{\text{Li}} + m_{\text{M}}}{m_{\text{M}}}\mu_{\text{V}}\right) \geq 0. \quad (20)$$

The equality sign holds in equilibrium, where the entropy production assumes its minimum value zero. In non-equilibrium the production of entropy must be positive. Thus in equilibrium we have  $f_{\text{Li}} = 0$  and  $\nabla(\mu_{\text{Li}} - (m_{\text{Li}} + m_{\text{M}})/m_{\text{M}} \mu_{\text{V}}) = 0$ .

The most simple possibility to satisfy the entropy inequality in non-equilibrium is given by Fick's law

$$f_{\text{Li}} = -M_{\text{B}}(T, y)\nabla\left(\mu_{\text{Li}} - \frac{m_{\text{Li}} + m_{\text{M}}}{m_{\text{M}}}\mu_{\text{V}}\right), \quad (21)$$

where the bulk mobility satisfies  $M_{\text{B}}(T, y) > 0$ .

Note that the entropy inequality holds point-wise, thus there is also an inequality at the interface  $I$ , viz.

$$-\rho(v^\nu - w^\nu)\left[\psi + \frac{1}{2}(v - w)^2\right] + [[\sigma^{ij}(v^i - w^i)]]\nu^j - [[\mu_{\text{Li}}f_{\text{Li}}^\nu + \mu_{\text{V}}f_{\text{V}}^\nu]] \geq 0. \quad (22)$$

The derivation of the entropy inequalities (20) and (22) are found to be in [4] and [3]. In particular details concerning the treatment of vacancies and side conditions are given there.

The interfacial entropy production will be used to formulate relations that are similar to Fick's law in the bulk phases. To this end we bring the left hand side of (22) by means of  $\sigma^{ij} = -p\delta^{ij}$ , the flux definitions (11), (12) and (7), the conservation laws (8), the Gibbs-Duhem relation (19)<sub>4</sub> and the identities (13) and (14) into a more appropriate form:

$$\dot{\mathcal{N}}_{\text{Li}}\left[[\mu_{\text{Li}} - \mu_{\text{V}} + \frac{m_{\text{Li}}}{2}(v - w)^2\right] + \dot{\mathcal{N}}_{\text{M}}\left[[\mu_{\text{V}} + \frac{m_{\text{M}}}{2}(v - w)^2\right] \geq 0. \quad (23)$$

Note the similarity between (20) and (23). In any case the entropy production is a sum of products *flux*  $\times$  *driving force*. In (20) the flux is the diffusion flux of Li and the driving force has to be identified with the gradient of a chemical potential difference. At the interface two products contribute to the entropy production: The flux of the first contribution is the atomic Li flux across the interface and the jump of the chemical potential difference plus a kinetic contribution is the driving force. The flux of the second product is identified as the atomic FePO<sub>4</sub> flux and the driving force is the jump consisting of the chemical potential of the vacancies plus a kinetic contribution. The both kinetic contributions are often small in comparison with the chemical potentials.

The equality sign of (23) holds in equilibrium and in non-equilibrium the interfacial entropy production must be positive. Thus in equilibrium we have  $\dot{\mathcal{N}}_{\text{Li}} = 0$  and  $\dot{\mathcal{N}}_{\text{M}} = 0$ , and the possible equilibria are determined by

$$[[\mu_{\text{Li}} - \mu_{\text{V}}]] = 0 \quad \text{and} \quad [[\mu_{\text{V}}]] = 0. \quad (24)$$

In an analogous manner to the bulk, the simplest possibility to satisfy the interfacial entropy production in equilibrium as well as in non-equilibrium is given by the ansatz

$$\dot{\mathcal{N}}_{\text{Li}} = M_{\text{I}}^{Li} \left[ [\mu_{\text{Li}} - \mu_{\text{V}} + \frac{m_{\text{Li}}}{2}(v-w)^2] \right], \quad \text{and} \quad \dot{\mathcal{N}}_{\text{M}} = M_{\text{I}}^M \left[ [\mu_{\text{V}} + \frac{m_{\text{M}}}{2}(v-w)^2] \right]. \quad (25)$$

Thus there are two positive mobilities at the interface, viz.  $M_{\text{I}}^{Li}$  and  $M_{\text{I}}^M$ .

We may conclude from the results of this section that if we were to know the free energy density, we could calculate all the other constitutive quantities. However, the bulk mobility and the two interfacial mobilities must be determined either by statistical thermodynamics or by experiments.

### 3.4 Constitutive law, Part2: Explicit forms of the pressure, free energy density and chemical potentials

The strategy to determine the specific free energy, i.e. the two functions  $\hat{\psi}(T, n_{\text{Li}}, n_{\text{V}})$  and  $\tilde{\psi}(T, y, \rho)$ , is as follows: At first we use (19)<sub>3</sub> to determine the  $\rho$  dependence of the function  $\psi$ , which is given by the pressure. Therefore we start with a constitutive law that relates the pressure to the volume change of the matrix lattice. We assume

$$p = \bar{p} + K \left( \frac{n_{\text{M}}}{\bar{n}_{\text{M}}} - h(y) \right) \quad \text{with} \quad h(y) = \frac{1}{1 + y\delta}. \quad (26)$$

Here  $\bar{n}_{\text{M}}$  denotes the particle density of  $\text{FePO}_4$  in the undeformed reference state of the matrix lattice. The bulk modulus is denoted by  $K$ . According to [9],  $K$  depends on the Li fraction  $y$ , but we ignore that fact in the simplified model. The function  $h(y)$  describes the phenomenon that Li atoms need more space than the vacancies. If  $\delta = 0$  we were to have  $n_{\text{M}} = \bar{n}_{\text{M}}$  at  $p = \bar{p}$ . However, there is a volumetric expansion  $(V - \bar{V})/\bar{V}$  of the host system if the Li fraction changes from 0 to 1. We denote its maximum for  $y = 1$  by  $\delta \equiv (V_{\text{max}} - \bar{V})/\bar{V}$ , which is about 0.06. For other values of  $y$  we simply interpolate and write  $(V - \bar{V})/\bar{V} = y\delta$ . The volume expansion is measured at the reference pressure, where we have  $n_{\text{M}}/\bar{n}_{\text{M}} = h(y)$ , on the other hand  $n_{\text{M}}/\bar{n}_{\text{M}} = \bar{V}/V$ , therefore we obtain  $h(y)$  as it is given by (26)<sub>2</sub>.

Next we apply (19)<sub>3</sub> to calculate the mechanical part of the free energy from the pressure. Since the derivative of the function  $\tilde{\psi}$  depends on the variables  $y$  and  $\rho$ , we represent  $p$  in the same variables, and we integrate

$$\frac{\partial \tilde{\psi}}{\partial \rho} = \frac{p}{\rho^2} = \frac{\bar{p} - Kh(y)}{\rho^2} + \frac{K}{\bar{n}_{\text{M}}m(y)} \frac{1}{\rho}. \quad (27)$$

We obtain

$$\rho \tilde{\psi}(T, y, \rho) = (\bar{p} - Kh(y)) \left( \frac{\rho}{\bar{n}_{\text{M}}m(y)h(y)} - 1 \right) + K \frac{\rho}{\bar{n}_{\text{M}}m(y)} \log \left( \frac{\rho}{\bar{n}_{\text{M}}m(y)h(y)} \right) + \frac{\rho}{m(y)} C(T, y). \quad (28)$$

We have chosen the integration constant so that the remaining unknown function  $C(T, y)$  can be identified with the chemical part of the free energy density, which is defined by

$$C(T, y) \equiv \tilde{\psi}^{\text{chem}}(T, y) \equiv \tilde{\psi}(T, y, \bar{n}_{\text{M}}m(y)h(y)). \quad (29)$$

The definition of the chemical part relies on the fact that this part is determined at constant reference pressure, which is guaranteed by the definition (29). We now can also define the mechanical part of the free energy density by

$$\rho\psi^{\text{mech}} \equiv \rho\psi - \rho\psi^{\text{chem}}, \quad (30)$$

and we conclude that the first two terms on the right hand side of (28) give  $\rho\psi^{\text{mech}}$ .

The motivation of that decomposition relies on the fact, that our knowledge on the two contributions to the free energy originates from different sources. The chemical part can be calculated within statistical thermodynamics, and the simplest model that is capable to exhibit two coexisting phases is given by, see also the phase field approach by Han et. al. [8] where the same function is used,

$$\rho\psi^{\text{chem}} = n_{\text{M}}\Omega \left( y(1-y) + \frac{kT}{\Omega} (y \log(y) + (1-y) \log(1-y)) \right) \equiv n_{\text{M}}\Omega f(y). \quad (31)$$

The first term gives an energetic contribution whose strength is controlled by the constant  $\Omega > 0$ , whereas the second contribution is purely entropic.  $k$  denotes the Boltzmann constant. Note that the positivity of  $\Omega$  may lead to a non-convex function, which is necessary to obtain two coexisting phases.

Thus the free energy density for the host system can be written as

$$\rho\psi = \Omega n_{\text{M}}f(y) + (\bar{p} - Kh(y)) \left( \frac{n_{\text{M}}}{\bar{n}_{\text{M}}h(y)} - 1 \right) + K \frac{n_{\text{M}}}{\bar{n}_{\text{M}}} \log\left(\frac{n_{\text{M}}}{\bar{n}_{\text{M}}h(y)}\right) \quad (32)$$

Next we calculate the chemical potentials. According to (19)<sub>1</sub> and (19)<sub>2</sub> we need the identities

$$\frac{\partial n_{\text{M}}}{\partial n_{\text{Li}}} = 1, \quad \frac{\partial n_{\text{M}}}{\partial n_{\text{V}}} = 1, \quad \frac{\partial y}{\partial n_{\text{Li}}} = \frac{1-y}{n_{\text{M}}}, \quad \frac{\partial y}{\partial n_{\text{V}}} = -\frac{y}{n_{\text{M}}}. \quad (33)$$

We obtain for Li

$$\begin{aligned} \frac{1}{\Omega}\mu_{\text{Li}} &= f + (1-y)f' + \\ & a_1 \left( \log\left(\frac{n_{\text{M}}}{\bar{n}_{\text{M}}h}\right) - \frac{h'}{h} \left(1 - \frac{\bar{n}_{\text{M}}h}{n_{\text{M}}}\right) (1-y) \right) + a_2 \left( 1 - \frac{h'}{h} (1-y) \right) \frac{1}{h}, \end{aligned} \quad (34)$$

and for the vacancies

$$\frac{1}{\Omega}\mu_{\text{V}} = f - yf' + a_1 \left( \log\left(\frac{n_{\text{M}}}{\bar{n}_{\text{M}}h}\right) + \frac{h'}{h} \left(1 - \frac{\bar{n}_{\text{M}}h}{n_{\text{M}}}\right) y \right) + a_2 \left( 1 + \frac{h'}{h} y \right) \frac{1}{h}. \quad (35)$$

The newly introduced constants  $a_1 = K/\bar{n}_{\text{M}}\Omega$  and  $a_2 = \bar{p}/\bar{n}_{\text{M}}\Omega$  control the strength of mechanical in comparison to chemical driving forces.

## 4 The model for infinite bulk diffusivity and spherical symmetry

In this section we exploit the thermodynamic model for the host system under some assumptions that will drastically simplify the analysis. The general case will be treated in a forthcoming study.

### 4.1 Simplifying assumptions

Recall that the model contains three inherent time scales, and a fourth time scale is given by the boundary conditions. These scales can be extracted from the mobility in the bulk,  $M_B$ , the mobilities for interfacial kinetics,  $M_{Li}^I$  and  $M_M^I$ , and the speed of supply and removal of Li atoms at the outer boundary. Relying on data found in [8], we now assume that the fastest of these processes is diffusion in the bulk, and we consider the limiting case of infinite bulk mobility. In other words: For finite diffusion flux and infinite bulk mobility, the chemical potentials and thus the number densities of the constituents become homogeneous within the two phases, because Fick's law (21), viz.  $f_{Li} = -M_B \nabla(\mu_{Li} - (m_{Li} + m_M)/m_M \mu_V)$ , assumes the form  $f_{Li} = -\infty \times 0$  and thus cannot be used anymore to determine the diffusion flux in this limiting case. In fact we shall see that for infinite bulk mobility  $f_{Li}$  follows from the local conservation law for the Li content.

In Section 3.4 we have already ignored the orthorhombic symmetry of the matrix lattice and the deviatoric stress components, so that the constitutive law (26) for the pressure is sufficient to describe the deformation of the lattice.

A further assumption concerns the geometric shape of the host system and of the interface I. We assume that the host system is a sphere with outer time dependent radius  $r_0(t)$ , and the morphology of the distribution of the two phases is an inner core  $\Omega_-$  with interfacial radius  $r_I$  and an outer shell  $\Omega_+$ . It is important to note that this assumption has been criticized by Allen et. al., see [1], and we shall devote a further study to their reasonings.

Finally we have to fix the location  $r_I(t_0)$  where the interface starts when we enter into the 2-phase region. Loading and unloading of the host system with Li atoms happens at the outer boundary. Despite the idealized assumption of homogeneity of the densities in bulk, it is obvious that if we reach the 2-phase region by supply of Li at  $r_0$ , the Li fraction will be slightly larger here than in the interior, so that the interface will start at the outer boundary for the loading process. On the other, the interface will also start at the outer boundary if we approach the 2-phase region during unloading of Li, because in that case the Li fraction at  $r_0$  will obviously be slightly smaller than in the interior.

## 4.2 Conservation laws of particle numbers

For spherical symmetry the relevant conservation laws of particle numbers (5) read in regular points of the bulk phases

$$\frac{\partial n_M}{\partial t} + \frac{1}{r^2} \frac{\partial r^2 n_M v_M}{\partial r} = 0 \quad \text{and} \quad \frac{\partial n_{\text{Li}}}{\partial t} + \frac{1}{r^2} \frac{\partial r^2 n_{\text{Li}} v_{\text{Li}}}{\partial r} = 0, \quad (36)$$

and in singular points on the interface we have from (6)

$$n_M^+(v_M^+ - \dot{r}_I) = n_M^-(v_M^- - \dot{r}_I) \quad \text{and} \quad n_{\text{Li}}^+(v_{\text{Li}}^+ - \dot{r}_I) = n_{\text{Li}}^-(v_{\text{Li}}^- - \dot{r}_I). \quad (37)$$

The boundary conditions that we need to exploit these equations are

$$\lim_{r \rightarrow 0} r^2 v_{M,\text{Li}} = 0, \quad v_M(t, r_0(t)) = \dot{r}_0(t), \quad j(t, r_0(t)) = j_0(t). \quad (38)$$

The function  $\dot{r}_0(t)$  follows from the solution of the mechanical part of the problem, see the next section, while the external Li flux  $j_0(t)$  can be related to the electric current. This latter boundary condition motivates to substitute the Li velocity  $v_{\text{Li}}$  by the Li flux according to  $v_{\text{Li}} = j + n_{\text{Li}} v_M$ .

The boundary condition (38)<sub>3</sub> indicates that the host system is an open system for Li. However, the total number  $N_M$  of  $\text{FePO}_4$  particles is conserved, and we can formulate its global conservation law  $N_M = N_M^- + N_M^+$ , which reads more explicitly for the simplified case at hand

$$\bar{n}_M \bar{r}_0^3 = n_M^- r_I^3 + n_M^+ (r_0^3 - r_I^3). \quad (39)$$

Recall that  $\bar{n}_M$  is the density of  $\text{FePO}_4$  particles in the deformation free reference state, i.e.  $y = 0$  and  $p = \bar{p}$ . The outer radius of the host system in this state is denoted by  $\bar{r}_0$ .

Due to the homogeneity assumption, the densities  $n_M(t)$  and  $n_{\text{Li}}(t)$  depend only on time, thus we may simply integrate the conservation laws (36) to obtain

$$r^2 n_M v_M(t, r) = -\dot{n}_M \frac{r^3}{3} + a(t) \quad \text{and} \quad r^2 j(t, r) = -n_M \dot{y} \frac{r^3}{3} + b(t). \quad (40)$$

The functions  $a(t)$  and  $b(t)$  are determined by the boundary conditions (38) and they assume different values in  $\Omega_+$  and  $\Omega_-$ . They will be determined by the four boundary condition (38) to obtain in  $\Omega_-$

$$n_M^- v_M^-(t, r) = -\frac{1}{3} \dot{n}_M^- r \quad \text{and} \quad j^-(t, r) = -\frac{1}{3} n_M^- \dot{y}^- r, \quad (41)$$

and in  $\Omega_+$  we have

$$r^2 n_M^+ v_M^+(t, r) = r_0^2 n_M^+ \dot{r}_0 + \frac{1}{3} \dot{n}_M^+ (r_0^3 - r^3) \quad \text{and} \quad r^2 j^+(t, r) = r_0^2 j_0 + \frac{1}{3} n_M^+ \dot{y}^+ (r_0^3 - r^3). \quad (42)$$

Next we exploit the jump conditions (37). We start with (37)<sub>2</sub>, which may be written as

$$j^+ - j^- + (y^+ - y^-)n_{\text{M}}^-(v_{\text{M}}^- - \dot{r}_{\text{I}}) = 0. \quad (43)$$

The fluxes  $j^+$  and  $j^-$  will be eliminated by means of (41)<sub>2</sub> and (42)<sub>2</sub>, and after use of the conservation law (39) we obtain

$$3r_0^2 j_0 + n_{\text{M}}^+ \dot{y}^+ (r_0^3 - r_{\text{I}}^3) + n_{\text{M}}^- \dot{y}^- r_{\text{I}}^3 - (y^+ - y^-)(n_{\text{M}}^- r_{\text{I}}^3) = 0. \quad (44)$$

Now we may use (39) once more to substitute the factor of  $\dot{y}^+$  so that after some simple rearrangements (44) reduces to

$$3r_0^2 j_0 + \frac{d}{dt} (\bar{n}_{\text{M}} \bar{r}_0^3 y^+ - (y^+ - y^-) n_{\text{M}}^- r_{\text{I}}^3) = 0. \quad (45)$$

This form of the Stefan condition can easily be integrated, and the final result is

$$\bar{n}_{\text{M}} \bar{r}_0^3 y^+(t) - (y^+(t) - y^-(t)) n_{\text{M}}^-(t) r_{\text{I}}^3(t) = \tilde{q}(t), \quad (46)$$

where the source function  $\tilde{q}(t)$  is defined by

$$\tilde{q}(t) \equiv - \int_{t_0}^t 3r_0^2 j_0(\tau) d\tau + \bar{n}_{\text{M}} \bar{r}_0^3 y^+(t_0) - (y^+(t_0) - y^-(t_0)) n_{\text{M}}^-(t_0) r_{\text{I}}^3(t_0). \quad (47)$$

### 4.3 The mechanical problem

The mechanical problem which is formulated in Section 3.2 reads in radial coordinates

$$\frac{\partial p}{\partial r} = 0 \quad \text{for } r \in \Omega_{+/-}(t) \quad \text{and} \quad p^- - p^+ = \frac{2\gamma}{r_{\text{I}}} \quad \text{for } r = r_{\text{I}}(t). \quad (48)$$

From (48)<sub>1</sub> we conclude

$$p = p^+(t) \quad \text{for } r \in \Omega_+(t) \quad \text{and} \quad p = p^-(t) \quad \text{for } r \in \Omega_-(t). \quad (49)$$

There are two cases possible that lead to different boundary conditions at the outer boundary  $r = r_0(t)$ .

Case 1: The outer pressure  $p_0$  is fixed, i.e.  $p^+ = p_0$ . In that case the outer radius  $r_0$  changes in fact with time and must be calculated from the conservation law (39).

Case 2: The external radius  $r_0$  is fixed, i.e.  $r = r_0$ . In that case the pressure  $p^+ = p_0(t)$  changes with time and must be calculated from the constitutive law (26).

At first we exploit the pressure controlled Case 1. We insert the constitutive law (26) into  $p^+ = p_0$  and into the interfacial condition (48)<sub>2</sub> to obtain

$$n_{\text{M}}^+ = \bar{n}_{\text{M}}(h(y^+) + \frac{1}{K}(p_0 - \bar{p})) \quad \text{and} \quad n_{\text{M}}^- = \bar{n}_{\text{M}}(h(y^-) + \frac{1}{K}(p_0 - \bar{p} + \frac{2\gamma}{r_{\text{I}}}). \quad (50)$$

Finally we solve the conservation law (39) for  $r_0(t)$ ,

$$r_0^3 = \frac{1}{n_M^+} (\bar{n}_M \bar{r}_0^3 + (n_M^+ - n_M^-) r_I^3). \quad (51)$$

Thus we are able to eliminate  $n_M^+$  and  $n_M^-$  in the chemical potentials, see (34) and (35), and we end up with chemical potentials that depend on the Li fractions  $y^-$ ,  $y^+$  and on the interfacial radius  $r_I$ .

In an analogous manner we treat the volume controlled Case 2. Here the resulting density of the matrix constituent reads in  $\Omega_+$

$$n_M^+ = \frac{\bar{n}_M \bar{r}_0^3}{r_0^3} (1 + (h(y^+) - h(y^-)) (\frac{r_I}{\bar{r}_0})^3 - \frac{2\gamma}{K} (\frac{r_I}{\bar{r}_0})^2), \quad (52)$$

and in  $\Omega_-$  we have

$$n_M^- = \frac{\bar{n}_M \bar{r}_0^3}{r_0^3} (1 + (h(y^+) - h(y^-)) ((\frac{r_0}{\bar{r}_0})^3 - (\frac{r_I}{\bar{r}_0})^3) + \frac{2\gamma}{K} \frac{1}{r_I} ((\frac{r_0}{\bar{r}_0})^3 - (\frac{r_I}{\bar{r}_0})^3)). \quad (53)$$

For fixed  $r_0$ , the pressure  $p_0$  depends on time, and this dependence is obviously given by

$$p_0 = \bar{p} + K (\frac{n_M^+(t)}{\bar{n}_M} - h(y^+(t))). \quad (54)$$

Note that the possibility to treat the mechanical problem independent of the diffusion problem is an extraordinary case, which is met here because we have ignored deviatoric stresses, so that the stress tensor reduces to a pressure. In the general case diffusion and mechanics must be solved simultaneously.

## 4.4 Evolution equations

Finally we exploit the evolution equations (25) for spherical symmetry. In this case it is easy to show by means of the definitions (7) that we have

$$\dot{\mathcal{N}}_{\text{Li}}^- = \frac{1}{4\pi r_I^2} \frac{d}{dt} (n_M^- y^- \frac{4\pi}{3} r_I^3) \quad \text{and} \quad \dot{\mathcal{N}}_M^- = \frac{1}{4\pi r_I^2} \frac{d}{dt} (n_M^- \frac{4\pi}{3} r_I^3). \quad (55)$$

We insert these identities into the left hand sides of the kinetic relations (25) and obtain

$$\frac{r_I}{3} \frac{d}{dt} (n_M^- y^-) + n_M^- y^- \frac{dr_I}{dt} = M_I^{\text{Li}} [[\mu_{\text{Li}} - \mu_V + \frac{m_{\text{Li}}}{2} (v - w)^2]], \quad (56)$$

$$\frac{r_I}{3} \frac{dn_M^-}{dt} + n_M^- \frac{dr_I}{dt} = M_I^{\text{M}} [[\mu_V + \frac{m_{\text{M}}}{2} (v - w)^2]]. \quad (57)$$

These equations and the integrated Stefan condition (46) determine the evolution of the interface radius  $r_I$  and of the atomic Li fractions  $y^{+/-}$ . To this end, however, one has to eliminate  $n_M^{+/-}$  by means of (50) for fixed external pressure  $p_0$  or with (52), (53) for fixed external radius  $r_0$ .



## 4.5 Dimensionless quantities

We introduce dimensionless quantities by means of the time scale of the external flux,  $t_0$ , and the radius  $\bar{r}_0$  of the host system for  $y = 0$ ,

$$\tau \equiv \frac{t}{t_0}, \quad \xi_{\text{I}} \equiv \frac{r_{\text{I}}}{\bar{r}_0}, \quad \xi_0 \equiv \frac{r_0}{\bar{r}_0}. \quad (58)$$

The dimensionless internal time scales are defined by

$$\tau_{\text{Li}} \equiv \frac{\bar{n}_{\text{M}}\bar{r}_0}{M_{\text{Li}}^{\text{I}}\Omega}, \quad \tau_{\text{M}} \equiv \frac{\bar{n}_{\text{M}}\bar{r}_0}{M_{\text{M}}^{\text{I}}\Omega}. \quad (59)$$

Furthermore we define dimensionless versions of the density of the matrix lattice, the diffusion flux, chemical potentials, the surface tension, the bulk modulus, and the external pressure, viz.

$$\nu \equiv \frac{n_{\text{M}}}{\bar{n}_{\text{M}}}, \quad J \equiv \frac{\bar{r}_0\bar{n}_{\text{M}}}{t_0}j, \quad \tilde{\mu} \equiv \frac{\mu}{\Omega}, \quad \tilde{\gamma} \equiv \frac{\gamma}{\bar{p}\bar{r}_0}, \quad \tilde{K} \equiv \frac{K}{\bar{p}}, \quad P \equiv \frac{p_0}{\bar{p}} - 1. \quad (60)$$

## 4.6 Summary

For fixed external pressure  $P$  we now give the explicit evolution system and initial and boundary data in dimensionless quantities for the three variables  $y^{+/-}$  and  $\xi_{\text{I}}$ . The case of fixed external radius  $\xi_0$  will be exploited in a further paper.

The evolution equations rely on the ODE system (56) and (57). The appearing kinetic energies are small for the case at hand and thus can be ignored. After some simple rearrangements we have

$$\frac{1}{3}\nu^-\xi_{\text{I}}\frac{dy^-}{dt} = \frac{1}{\tau_{\text{Li}}}(\mu^+ - \mu^-) - y^-\frac{1}{\tau_{\text{M}}}(\mu_{\text{V}}^+ - \mu_{\text{V}}^-), \quad (61)$$

$$\nu^-(\nu^- - \frac{1}{3}\frac{2\gamma}{K}\frac{1}{\xi_{\text{I}}})\frac{d\xi_{\text{I}}}{dt} = \delta\frac{1}{\tau_{\text{Li}}}(\mu^+ - \mu^-) + (\nu^- - y^-\delta)\frac{1}{\tau_{\text{M}}}(\mu_{\text{V}}^+ - \mu_{\text{V}}^-). \quad (62)$$

The integrated Stefan condition (46) serves to determine  $y^+$  according to

$$y^+ = \frac{q - y^-\nu^-\xi_{\text{I}}^3}{1 - y^-\nu^-\xi_{\text{I}}^3}, \quad (63)$$

where the source function

$$q(\tau) \equiv - \int_{\tau_0}^{\tau} 3\xi_0^2 J_0(\tilde{\tau})d\tilde{\tau} + y^+(\tau_0) - (y^+(\tau_0) - y^-(\tau_0))\nu^-(\tau_0)\xi_{\text{I}}^3(\tau_0) \quad (64)$$

contains the Li flux across the external boundary and initial data. It is easy to show that  $q(t)$  is the ratio of the total number of Li atoms and the total number of interstitial lattice sites, i.e.  $q(t) = N_{\text{Li}}(t)/N_{\text{M}}$ . The solution of the mechanical problem provides the dimensionless densities of the matrix particles in  $\Omega_{+/-}$

$$\nu^+ = h(y^+) + \frac{1}{K}P \quad \text{and} \quad \nu^- = h(y^-) + \frac{1}{K}(P + \frac{2\gamma}{\xi_{\text{I}}}), \quad (65)$$

and the dimensionless external radius

$$\xi_0^3 = \frac{1}{\nu^+} (1 + (\nu^+ - \nu^-) \xi_1^3), \quad (66)$$

which changes with time for fixed external pressure.

For completeness we also write down the density of matrix particles for the case of fixed volume. Recall that we shall not exploit this case here.

$$\nu^+ = (1 + (h(y^+) - h(y^-)) \xi_1^3 - \frac{2\gamma}{K} \xi_1^2), \quad (67)$$

$$\nu^- = (1 + (h(y^+) - h(y^-)) (\xi_0^3 - \xi_1^3) + \frac{2\gamma}{K} \frac{1}{\xi_1} (\xi_0^3 - \xi_1^3)). \quad (68)$$

Finally we give the chemical potentials  $\mu \equiv \mu_{\text{Li}} - \mu_{\text{V}}$  and  $\mu_{\text{V}}$  in terms of the dimensionless variables:

$$\mu = f'(y) - a_1 \frac{h'(y)}{h(y)} \left(1 - \frac{h(y)}{\nu}\right) - a_2 \frac{h'(y)}{h(y)^2}, \quad (69)$$

$$\mu_{\text{V}} = f(y) - yf'(y) + a_1 \left( \log\left(\frac{\nu}{h(y)}\right) + \frac{h'(y)}{h(y)} \left(1 - \frac{h(y)}{\nu}\right) y \right) + a_2 \left(1 + \frac{h'(y)}{h(y)} y\right) \frac{1}{h(y)}, \quad (70)$$

The functions  $h$  and  $\nu$  account for the mechanical contributions to the chemical potentials. Note that from (65) we have different representations for  $\nu$  in  $\Omega_{+/-}$ , viz.  $\nu^+(P, y^+)$  and  $\nu^-(P, \xi_1, y^-)$ . Accordingly there result different functions that represent the chemical potentials in the two phases. For the case of fixed external pressure these are written as  $\mu^+(P, y^+)$ ,  $\mu^-(P, \xi_1, y^+)$  and  $\mu_{\text{V}}^+(P, y^+)$ ,  $\mu_{\text{V}}^-(P, \xi_1, y^-)$ . On the other hand, if we consider a fixed external radius  $\xi_0$ , we have  $\nu^{+/-}(\xi_0, \xi_1, y^+, y^-)$ , i.e. the both Li fractions appear in  $\nu^+$  as well as in  $\nu^-$  and thus the chemical potential functions exhibit the same behavior.

The system (61) - (70) is a closed system that will be used in the following to determine the evolution of the host system for given external pressure  $P$  and external Li flux  $J_0(\tau)$ .

## 5 Simulations

In this section we numerically study the proposed model (61) - (70). To this end we choose the following parameters as fixed:

The considered processes run at constant temperature  $T_0 = 293.2\text{K}$  and constant pressure  $\bar{p} = 1\text{bar}$ , i.e.  $P = 0$ . The atomic masses of Li and the matrix particles  $\text{FePO}_4$  are  $m_{\text{Li}} = 3$  and  $m_{\text{M}} = 105$ . The density of matrix particles is  $\bar{n}_{\text{M}} = 8.396 \cdot 10^{28} \text{particles/m}^3$ . The mechanical parameters bulk modulus, surface tension and maximal volume change are chosen as  $K = 7.5 \cdot 10^{10} \text{N/m}^2$ ,  $\gamma = 0.075 \text{N/m}$  and

$\delta = 0.06$ . The free energy contains the interaction energy  $\Omega = 94.4 \cdot 10^{-22} \text{J/atom}$  and the 3 parameters  $a_1 = kT_0/\Omega = 0.390$ ,  $a_2 = K/(\bar{n}_M\Omega) = 11.5$  and  $a_3 = \bar{p}/(\bar{n}_M\Omega) = 0.000115$ . Here  $k = 1.38 \cdot 10^{-23} \text{J/K}$  denotes the Boltzmann constant. We choose the time and length scale of the model by  $t_0 = 125664 \text{s}$  and  $\bar{r}_0 = 20 \cdot 10^{-9} \text{m}$ , which is the time scale of the external flux, respectively the radius of the host system for Li fraction  $y = 0$ .

The two relaxation times  $\tau_{\text{Li}}$  and  $\tau_{\text{V}}$  of the model are not known because they did not yet appear in the literature. However, we shall assume that they have values on a time scale which is much smaller than the time scale of the external flux, and in Section 5.3 we will introduce various choices of  $\tau_{\text{Li}}$  and  $\tau_{\text{V}}$  to show their influence on the evolution of the host system.

## 5.1 Chemical Potentials

At first we discuss some properties of the chemical potentials  $\mu \equiv \mu_{\text{Li}} - \mu_{\text{V}}$  and  $\mu_{\text{V}}$ . Figures 4 and 5 show the both potentials without and with mechanical contributions. The mechanical phenomena are due to surface tension and Li induced volume changes of the matrix lattice. If these are ignored we were to have  $\mu = f'(y)$  and  $\mu_{\text{V}} = f(y) - yf'(y)$  with  $f$  given by  $(31)_2$ . In this case the chemical potentials exclusively depend on the Li fraction  $y$ , which is represented by the red respectively green curve of Figure 4.

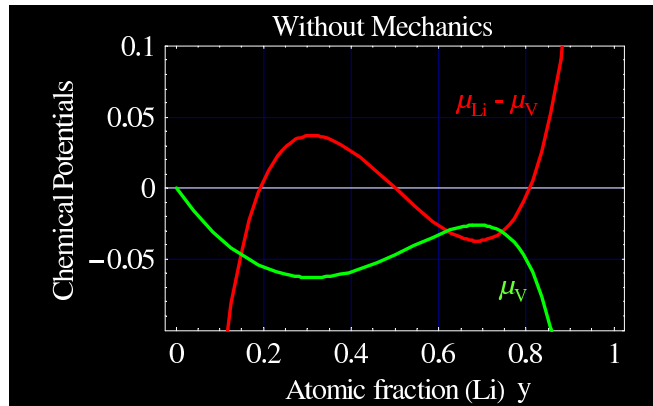


Figure 4: Relevant chemical potentials  $\mu = \mu_{\text{Li}} - \mu_{\text{V}}$  and  $\mu_{\text{V}}$  without mechanical contributions

If the mechanical phenomena are taken into account, the chemical potentials additionally depend on the location of the interface, i.e. on  $\xi_{\text{I}}$ . This dependence is illustrated in Figure 5 by the yellow and blue curves, which give the chemical potentials  $\mu$  and  $\mu_{\text{V}}$  for two different locations of the interface, viz.  $\xi_{\text{I}} = 0.43$  and  $\xi_{\text{I}} = 0.10$ .

The difference  $\mu = \mu_{\text{Li}} - \mu_{\text{V}}$  is not very much influenced by the location of the

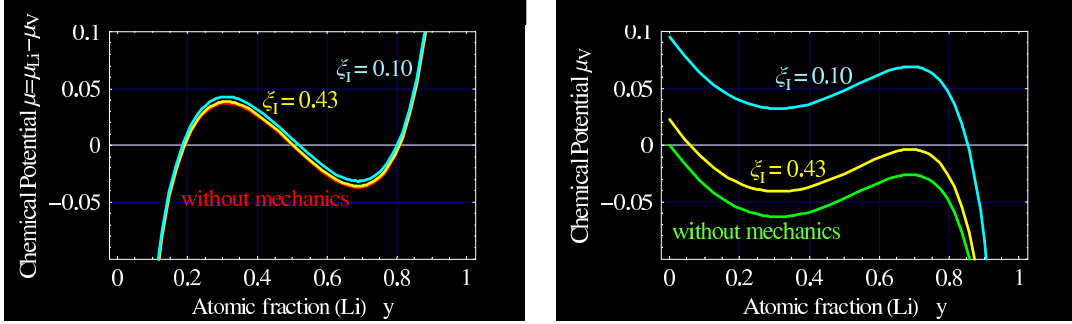


Figure 5: Red and green: Chemical Potentials as in Figure 4 without mechanical contributions. Yellow and blue: Chemical potentials with mechanical contributions for 2 different interfacial radii.

interface. This fact is important to understand the observed evolution of the voltage, which is determined by  $\mu$ . On the other hand, the chemical potential of the vacancies  $\mu_V$  depends quite sensitive on a variation of  $\xi_I$ . This fact is related to the origin of the hysteretic behavior of the charging/discharging process of the battery.

Finally we discuss the non-monotonicity of the chemical potentials. It is sufficient to consider the difference  $\mu$ . Let the Li fractions  $y_1 < y_2$  indicate the boundaries of the two regions  $0 \leq y < y_1$  and  $y_2 < y \leq 1$  where  $\mu$  is uniquely invertible with respect to  $y$ . If the total Li fraction  $q$  lies in either one of those ranges the Li distribution of the host system is represented by a single phase. For  $y_1 \leq q \leq y_2$ , there are three Li fractions corresponding to a given value of  $\mu$  and the host system may decompose into two phases which are separated by an interface. The explicit determination of the region where the Li distribution is represented by two adjacent phases is a subtle problem that will be solved in the next sections of this study.

## 5.2 Possible equilibria

In this section we determine the possible equilibria for given  $q$ , i.e. total fraction  $q$  of stored Li atoms.

The conditions for possible equilibria consists of the two equations (24), which guarantee zero interfacial entropy production,

$$\mu^+(P, y^+) = \mu^-(P, \xi_I, y^-) \quad \text{and} \quad \mu_V^+(P, y^+) = \mu_V^-(P, \xi_I, y^-), \quad (71)$$

and of the Stefan condition (63)

$$y^+ = \frac{q - y^- \nu^-(P, \xi_I, y^-) \xi_I^3}{1 - y^- \nu^-(P, \xi_I, y^-) \xi_I^3} \quad \text{with} \quad q = \frac{N_{\text{Li}}}{N_{\text{M}}}. \quad (72)$$

At first it is instructive to ignore the mechanical contributions. In that case, according to (69) and (70), the equations (71) reduce to the classical common tangent

construction

$$f'(y^+) = f'(y^-) \quad \text{and} \quad f(y^+) - y^+ f'(y^+) = f(y^-) - y^- f'(y^-), \quad (73)$$

which determine the so called Maxwell line. Up to a symmetry transformation the solution  $(y^+, y^-)$  of (73), which is indicated in Figure 6 by the two white dots, is unique. The symmetry of (73) implies that we may have  $y^+ > y^-$  as well as  $y^+ < y^-$ . Furthermore it is important to note that a variation of the location of the interface does not change the equilibrium. After (73) is solved for  $(y^+, y^-)$  we may use the equation (72) in the form  $q = (1 - \xi_1^3)y^+ + \xi_1^3 y^-$  to determine either the interface radius  $\xi_1$  or  $q$ , which gives the ratio of total number of Li atoms and total number of interstitial lattice sites.

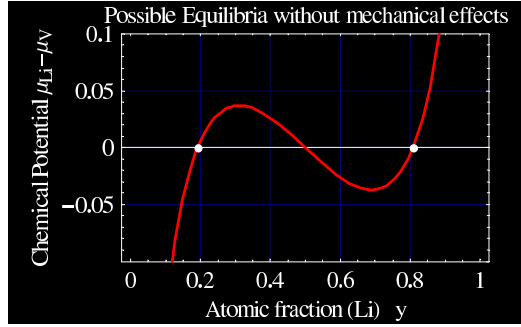


Figure 6:  $\mu = \mu_{\text{Li}} - \mu_V$  and the two equilibria  $y^+$  and  $y^-$  without mechanical contributions.

Next we include the mechanical phenomena into the discussion of the system (71), (72). In that case the radius  $\xi_1$  of the interface appears in (71), and thus the equilibria  $(y^+, y^-)$  depend on  $\xi_1$ .

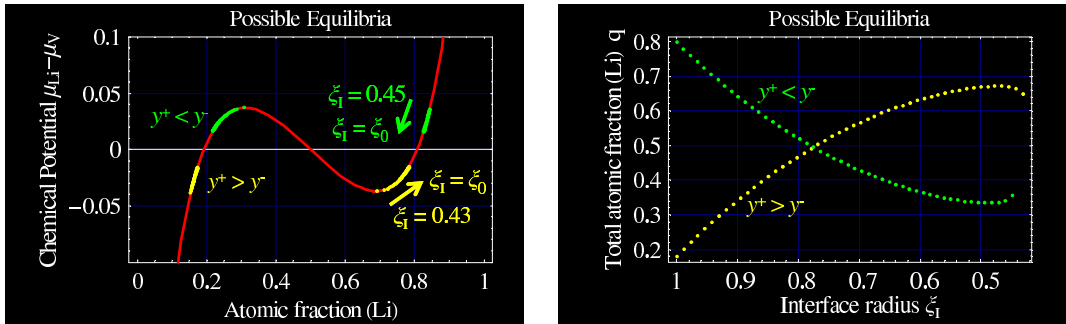


Figure 7: Possible equilibria when mechanical contributions are taken into account. Left:  $\mu = \mu_{\text{Li}} - \mu_V$  and possible equilibria  $(y^+, y^-)$  for  $y^+ > y^-$  (yellow) and for  $y^+ < y^-$  (green). Right : The corresponding interfacial radii  $\xi_1$  for given fixed total Li fraction.

There are two different compact domains of radii so that the triple  $(y^+, y^-, \xi_1)$  solves the equations (71), and (72) serves to calculate the corresponding prescribed total Li fraction  $q$ . The first domain contains the radii for which we have  $y^+ > y^-$ , while in the second domain  $y^+ < y^-$ . There is no symmetry anymore between the outer and inner region of the host system. From the left plot of Figure 7 we may read off the possible atomic Li fractions in equilibrium, which are indicated by dots with yellow color for  $y^+ > y^-$ , and with green color for  $y^+ < y^-$ .

The plot on the right hand side gives the corresponding interfacial radii for given total atomic Li fractions. It is important to note that for given  $q$  there is a region where two equilibria are possible. Which one is assumed by the host system for given initial data depends on the ratio of the relaxation times, see Table 1 in Section 5.4.

### 5.3 On the origin of the hysteretic behaviour

We assume that the host system approaches interfacial equilibrium on a much faster time scale than the loading respectively the unloading process. This assumption exhibits a hysteretic behavior of loading and unloading of the host system.

For a demonstration of this statement we use the data from Figure 7 and the equation (69) to establish a plot that gives the chemical potential  $-\mu^+ = -(\mu_{\text{Li}}^+ - \mu_{\text{V}}^+)$  versus the total electric charge of the cell shown in Figure 1, which is related to the total Li content of the host system by  $1 - q$ . If the electrolyte is treated as a liquid with infinite conductivity, it can be shown that the voltage  $U$  of the lithium cell is given by  $U = -1/e(\mu_{\text{Li}}^+ - \mu_{\text{V}}^+) + \text{const.}$ .

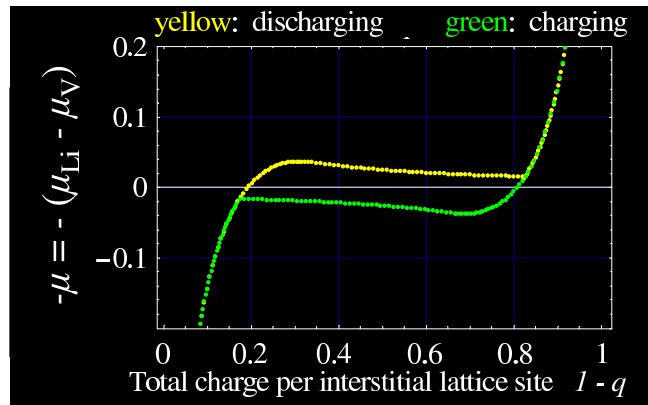


Figure 8: Hysteretic behaviour during charging (green) and discharging (yellow).

We now compare the calculated hysteresis plot of Figure 8 with the corresponding experimental data from Figure 2 and observe two essential differences. The experimentally observed horizontal branches exhibit in the model a slight negative slope, and the connections of the two-phase region to the single phase regions differ from the corresponding experimental data.

Various reasons for these discrepancies are possible. For example, in the current paper our first exploitation of the model relies on several simplifying assumptions, viz. (i) fast bulk diffusion in comparison with the interface evolution, (ii) the stress deviator and the anisotropy of the  $\text{FePO}_4$  lattice have been ignored, (iii) the dependence of the elastic coefficients on the Li fraction has been ignored, (iv) the shape of the interface is a sphere and (v) the hysteresis is generated via local equilibrium states.

Note that these five assumptions are not included in the general model that is proposed in this study. In fact we exclusively introduced those assumptions for an easy treatment of the simulations in this study. In a forthcoming paper we shall rely on the complete model as it is established here, and in particular we shall give a careful calibration of the model parameter to the experimental data. The main objective of the current study is to show that there is a thermodynamic model that is capable to describe and predict properties of the loading and unloading process of the host system by Li atoms.

## 5.4 Evolutions for various initial and boundary data

In this section we choose various initial and boundary data to study the subsequent evolution of the host system to the possible equilibrium states. The simulation is based on the ODE system (61), (62) and the algebraic equation (63) which brings via the source function  $q(\tau)$  an explicit time dependence into (61) and (62).

The variables are the Li fractions  $y^+(\tau)$ ,  $y^-(\tau)$  in the two regions  $\Omega^{+/-}$ , and the interface radius  $\xi_I(\tau)$ .

Here we consider a constant  $q = N_{\text{Li}}/N_{\text{M}}$ , i.e. the total content of Li atoms in the host system is constant during the evolution. In order to demonstrate the influence of the two relaxation times  $\tau_{\text{Li}}$  and  $\tau_{\text{V}}$  on the evolution we consider three cases, viz.

$$(\tau_{\text{Li}}, \tau_{\text{M}}) = (1, 1), \quad (\tau_{\text{Li}}, \tau_{\text{M}}) = (10^{-3}, 1), \quad \text{and} \quad (\tau_{\text{Li}}, \tau_{\text{M}}) = (1, 10^{-3}). \quad (74)$$

A careful examination of the system (61) and (62) reveals that  $\tau_{\text{M}}$  controls the evolution of the interface radius  $\xi_I$  and of the chemical potential difference  $\mu_{\text{V}}^+ - \mu_{\text{V}}^-$ , whereas the evolution of the ratio  $y^-/y^+$  is in first order determined by the value of  $\tau_{\text{Li}}$ .

Recall our assumption that during loading as well as during unloading the interface starts to appear at the outer radius with  $y^+ > y^-$  during loading respectively with  $y^+ < y^-$  during unloading. For this reason we consider initial data satisfying

$$\xi_I(0) = 0.99 \xi_0(0), \quad y^-(0) = \begin{cases} 0.95 y^+(0) & \text{loading,} \\ 1/0.95 y^+(0) & \text{unloading.} \end{cases} \quad \text{to simulate} \quad (75)$$

From the initial data (75) we calculate  $q(0) = q(t)$  by means of (63), and provide a list of ten values in the following table which describes the characteristics of the

evolution of the host system for the three pairs of relaxation times given by (74). We observe that three possible final states: The initially 2-phase system may end up as a single phase or in 2-phase equilibrium, which is indicated by the symbols 1 and 2, respectively. Furthermore the table gives the information whether the initial conditions  $y^+(0) > y^-(0)$  and  $y^+(0) < y^-(0)$  are conserved during the evolution. Recall that Figure 7 shows a region where two equilibria are possible for a given total amount of Li atoms. Which of these are assumed by the host system depends on the chosen relaxation times. For example, when the interface reaches the first possible equilibrium location, see Figure 7, but the ratio  $y^-/y^+$  needs more time to establish equilibrium, then the interface motion still goes on up to the second equilibrium location.

$q$	$y^+(0) > y^-(0)$			$q$	$y^+(0) < y^-(0)$		
	$(\tau_{Li}, \tau_M) = (1, 1)$	$(\tau_{Li}, \tau_M) = (10^3, 1)$	$(\tau_{Li}, \tau_M) = (1, 10^3)$		$(\tau_{Li}, \tau_M) = (1, 1)$	$(\tau_{Li}, \tau_M) = (10^3, 1)$	$(\tau_{Li}, \tau_M) = (1, 10^3)$
0.294381	1	1	1	0.294381	1	1	1
0.294391	1	2: $y^+ > y^-$	1	0.294391	1	2: $y^+ > y^-$	1
0.40	2: $y^+ > y^-$	2: $y^+ > y^-$	2: $y^+ < y^-$	0.40	2: $y^+ < y^-$	2: $y^+ < y^-$	2: $y^+ < y^-$
0.62	2: $y^+ > y^-$	2: $y^+ > y^-$	2: $y^+ < y^-$	0.62	2: $y^+ < y^-$	2: $y^+ < y^-$	2: $y^+ < y^-$
0.72	2: $y^+ < y^-$	1	2: $y^+ < y^-$	0.72	2: $y^+ < y^-$	1	2: $y^+ < y^-$
0.727694	2: $y^+ < y^-$	1	2: $y^+ < y^-$	0.727694	2: $y^+ < y^-$	1	2: $y^+ < y^-$
0.727704	1	1	2: $y^+ < y^-$	0.727704	2: $y^+ < y^-$	1	2: $y^+ < y^-$
0.758013	1	1	2: $y^+ < y^-$	0.758013	1	1	2: $y^+ < y^-$
0.758022	1	1	1	0.758022	1	1	2: $y^+ < y^-$
0.758610	1	1	1	0.758610	1	1	1

Table 1: Evolution of the host system for different initial data and relaxation times.

Finally we discuss a series of plots showing explicitly the evolution of the interface radius  $\xi_I(\tau)$ , the ratio  $y^-(\tau)/y^+(\tau)$  and of the four chemical potentials  $\mu^+(\tau)$ ,  $\mu^-(\tau)$ , indicated by red respectively orange color, and  $\mu_V^+(\tau)$ ,  $\mu_V^-(\tau)$ , indicated by blue and magenta. Thus the third plot in each row gives an instructive illustration how the equilibria of the 2-phase state is approached, which is given by  $\mu^+ = \mu^-$  and  $\mu_V^+ = \mu_V^-$ .

We start with  $(\tau_{Li}, \tau_M) = (1, 1)$ ,  $y^+(0) > y^-(0)$  and  $q = 0.294381$ , where only a single phase may exist in equilibrium. This is exhibited in Figure 9 where the interface ends up with  $\xi_I = 0$ .

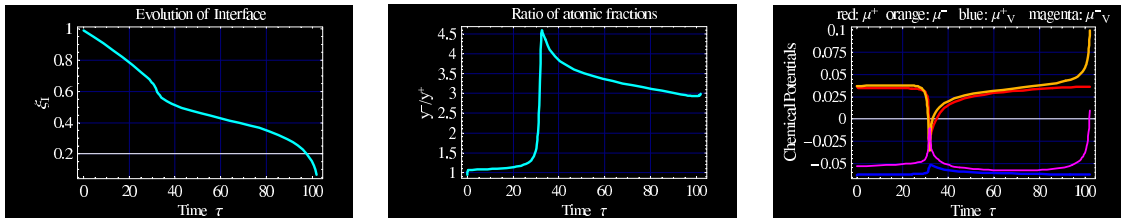


Figure 9: Evolution of the host system:  $(\tau_{Li}, \tau_M) = (1, 1)$ ,  $y^+(0) > y^-(0)$  and  $q = 0.294381$ .



The next three examples show the influence of different relaxation times on the evolution for the initial data  $y^+(0) > y^-(0)$  and  $q = 0.62$ . In each case we finally end up here with a 2-phase equilibrium. The initial condition  $y^+(0) > y^-(0)$  is conserved in Figures 10 and 11. Observe in Figure 11 that  $\mu = \mu_{\text{Li}} - \mu_{\text{V}}$  establishes much faster its equilibrium value  $\mu^+ = \mu^-$  than in Figure 10, which is due to the much smaller relaxation time  $\tau_{\text{Li}}$ . However, if  $\tau_{\text{V}}$  is the smallest relaxation time, the evolution drastically changes, which can be observed in Figure 12. In particular the initial condition  $y^+(0) > y^-(0)$  is not conserved here.

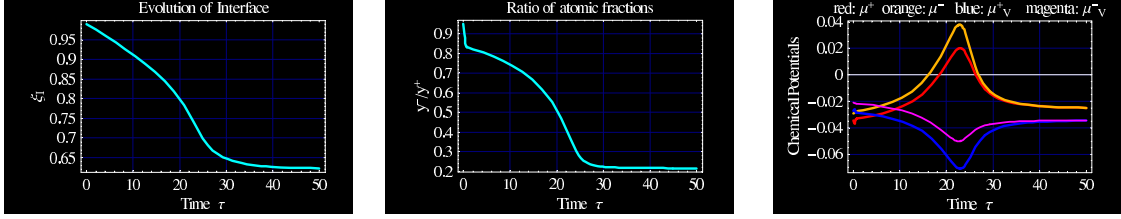


Figure 10: Evolution of the host system:  $(\tau_{\text{Li}}, \tau_{\text{M}}) = (1, 1)$ ,  $y^+(0) > y^-(0)$  and  $q = 0.62$

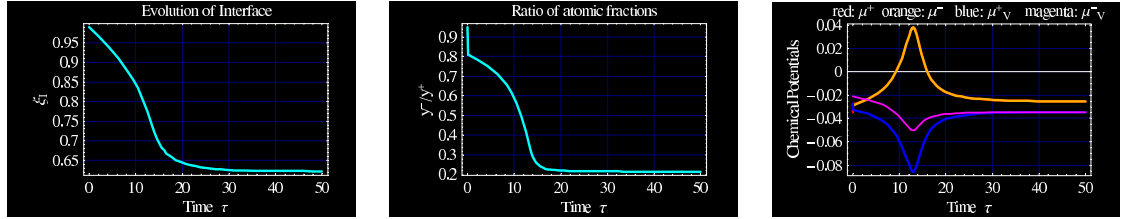


Figure 11: Evolution of the host system:  $(\tau_{\text{Li}}, \tau_{\text{M}}) = (10^{-3}, 1)$ ,  $y^+(0) > y^-(0)$  and  $q = 0.62$ .

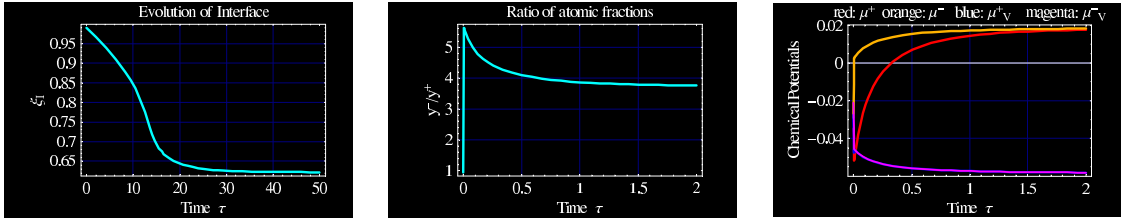


Figure 12: Evolution of the host system:  $(\tau_{\text{Li}}, \tau_{\text{M}}) = (1, 10^{-3})$ ,  $y^+(0) > y^-(0)$  and  $q = 0.62$

In the next three examples we change from total Li fraction  $q = 0.62$  to  $q = 0.72$  and consider again the case  $y^+(0) > y^-(0)$ , which now is only conserved in Figure 13 where we have  $\tau_{\text{Li}} = \tau_{\text{V}}$ . Figure 14, i.e.  $\tau_{\text{Li}} = 10^{-3} \tau_{\text{V}}$ , a 2-phase equilibrium is not possible, and this realized here by  $\xi_I \rightarrow 0$ . Finally we observe in Figure 15 a

non-monotone behavior of the interfacial radius and a very fast approach of  $\mu_V$  to its equilibrium value  $\mu_V^+ = \mu_V^-$ .

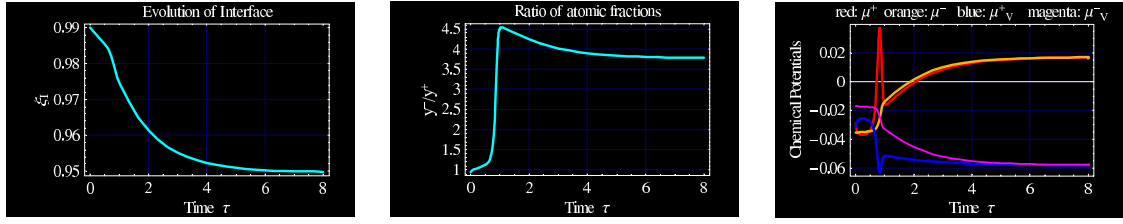


Figure 13: Evolution of the host system:  $(\tau_{\text{Li}}, \tau_{\text{M}}) = (1, 1)$ ,  $y^+(0) > y^-(0)$  and  $q = 0.62$

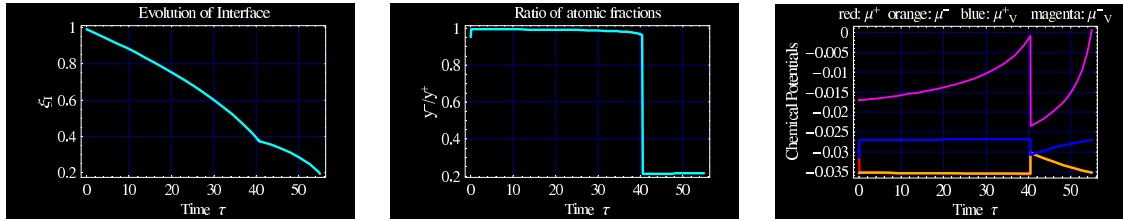


Figure 14: Evolution of the host system:  $(\tau_{\text{Li}}, \tau_{\text{M}}) = (10^{-3}, 1)$ ,  $y^+(0) > y^-(0)$  and  $q = 0.72$

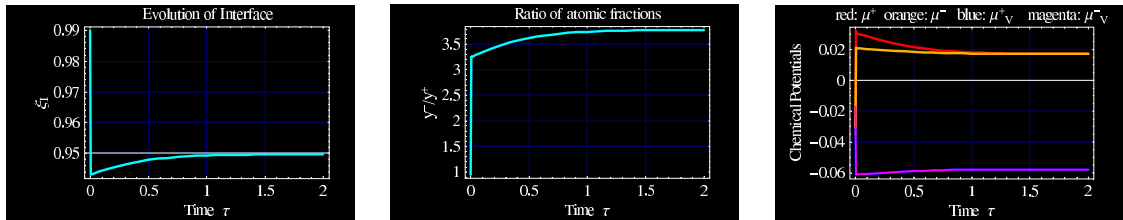


Figure 15: Evolution of the host system:  $(\tau_{\text{Li}}, \tau_{\text{M}}) = (1, 10^{-3})$ ,  $y^+(0) > y^-(0)$  and  $q = 0.72$

## 6 Appendix: Detailed description of motion, strain, stress and their influence on the chemical potentials

**Introduction.** In the current study we have described the deformation of the host system due to surface tension and Li induced volume changes of the crystal lattice within a simplified mechanical setting. In fact we have ignored that the host lattice

of the  $\text{Li}_y\text{FePO}_4$  particles have orthorhombic symmetry, so that 9 elastic constants are needed for a complete mechanical characterization. Furthermore we have ignored the deviatoric components of the stress, i.e. we have assumed the form  $\sigma^{ij} = -p\delta^{ij}$ .

In this section we shall give the necessary mechanical framework, i.e. we extend the constitutive theory of Sections 3.1 - 3.4. The application to the case at hand will be done in a forthcoming paper. For those readers who are interested in more details concerning the following statements we refer to [2] and [3]. The determination of the elastic constants of  $\text{Li}_y\text{FePO}_4$  and of the volume change due to lithiation is found to be in the recent study by Maxisch and Ceder [9].

**Motion, strain and stress.** At first we introduce a reference state in order to measure the motion of a material point of the  $\text{Li}_y\text{FePO}_4$  matrix. Let  $X = (X^i)_{i=1,2,3} = (X^1, X^2, X^3)$  be the location of a material point in a reference state, whose location at time  $t$  is given by  $x = (x^i)_{i=1,2,3} = (x^1, x^2, x^3)$ . The location  $x$  is determined by the function

$$x = \chi(t, X) = (\chi^1(t, X), \chi^2(t, X), \chi^3(t, X)). \quad (76)$$

We call  $\chi(t, X) = (\chi^i(t, X))_{i=1,2,3}$  the motion of the material points of the crystal, and the displacement of a material point at  $X$  is denoted by

$$U^i(t, X) = \chi^i(t, X) - X^i. \quad (77)$$

The motion can be used to calculate the velocity,  $\hat{v} = (\hat{v}^i)_{i=1,2,3}$ , and the deformation gradient,  $F = (F^{ij})_{i,j=1,2,3}$ , of the crystal:

$$\hat{v}^i(t, X) = \frac{\partial \chi^i(t, X)}{\partial t}, \quad F^{ij} = \frac{\partial \chi^i}{\partial X^j}. \quad (78)$$

We denote the Jacobian of  $F^{ij}$  by  $J$ , and we assume that  $J > 0$ , so that we may invert the motion  $x^i = \chi^i(t, X)$  at any time  $t$  with respect to the coordinates  $X^i$ . We write

$$X^i = (\chi^{-1})^i(t, x), \quad (79)$$

and define the displacement field  $u^i$  by

$$u^i(t, x) = U^i(t, \chi^{-1}(t, x)). \quad (80)$$

This is a typical example for the representation of mechanical quantities with respect to actual coordinates. We call this representation the Euler or the spatial description, whereas the representation with respect to the reference coordinates is called the Lagrange or material description.

The velocity  $\hat{v}^i(t, X)$  can likewise be given with respect to the coordinates  $x^i$ . We define  $v^i(t, x) \equiv \hat{v}^i(t, \chi^{-1}(t, x))$ , and we identify this quantity with the barycentric velocity that was introduced by (9)<sub>2</sub> in Section 3.1.

A similar definition for the mass density of the  $\text{Li}_y\text{FePO}_4$  particles, viz.  $\rho(t, x) = \hat{\rho}(t, \chi^{-1}(t, x))$ , is useful to integrate the mass balance (10)<sub>1</sub> to obtain

$$J = \det(F) = \frac{\bar{\rho}}{\rho}, \quad (81)$$

where  $\bar{\rho}$  is the mass density for  $F^{ij} = \delta^{ij}$ .

Further important objects for the description of the stretch are the right and the left Cauchy-Green tensor,  $C^{ij}$  and  $B^{ij}$ , and for the description of the strain we define the Green strain tensor  $G^{ij}$ :

$$C^{ij} = F^{mi} F^{mj}, \quad B^{ij} = F^{im} F^{jm}, \quad G^{ij} = \frac{1}{2}(C^{ij} - \delta^{ij}). \quad (82)$$

These quantities may also easily be given with respect to the spatial representation.

Next we decompose the stretch of a body into a part, which gives pure volume changes of the body and the complementary part, which describes pure changes of its shape. Pure changes of the volume are obviously given by the Jacobian  $J$ , whereas the unimodular tensor

$$c^{ij} \equiv J^{-2/3} C^{ij} \quad \text{with} \quad \det(\mathbf{c}) = 1 \quad (83)$$

represents changes of the shape of a body.

Furthermore we need to introduce two measures of stress: (i) the Cauchy stress  $\sigma^{ij} = \sigma^{ji}$ , which gives the actual force per actual surface element and (ii) the second Piola-Kirchhoff stress  $t^{ik}$ , which is defined by

$$t^{ij} = J(F^{-1})^{im}(F^{-1})^{jn}\sigma^{mn}. \quad (84)$$

The isotropic part of the Cauchy stress is related to the pressure  $p$ , which is defined by

$$p = -\frac{1}{3}\sigma^{mm}, \quad \text{so that} \quad \sigma^{ij} = -p\delta^{ij} + \sigma^{\langle ij \rangle} \quad \text{with} \quad \sigma^{\langle jj \rangle} = 0. \quad (85)$$

Here the angle brackets indicate the stress deviator, which represents the stress due to pure changes of the shape of a solid, whereas the pressure is related to pure changes of its volume.

**Free energy, chemical potentials and stress.** In the simplified mechanical treatment, the specific free energy relies on the representation (17):  $\psi = \hat{\psi}(T, n_{\text{Li}}, n_{\text{V}}) = \check{\psi}(T, y, \rho)$ . Its generalization to the complete mechanical description reads

$$\psi = \hat{\psi}(T, n_{\text{Li}}, n_{\text{V}}, c^{ij}) = \tilde{\psi}(T, y, \rho, c^{ij}) = \check{\psi}(T, y, C^{ij}). \quad (86)$$

The calculation of the chemical potentials and the pressure, which is now defined by  $p = -\sigma^{nn}/3$ , rely on the same rules as before, i.e. according to (19) we have

$$\mu_{\text{Li}} = \frac{\partial \rho \hat{\psi}}{\partial n_{\text{Li}}}, \quad \mu_{\text{V}} = \frac{\partial \rho \hat{\psi}}{\partial n_{\text{V}}}, \quad p = \rho^2 \frac{\partial \tilde{\psi}}{\partial \rho}, \quad \rho \psi + p = \mu_{\text{Li}} n_{\text{Li}} + \mu_{\text{V}} n_{\text{V}}, \quad (87)$$

and the function  $\check{\psi}(T, y, C^{ij})$  is used to calculate the 2<sup>nd</sup> Piola Kirchhoff stress by means of

$$t^{ij} = 2\bar{\rho} \frac{\partial \check{\psi}}{\partial C^{ij}}. \quad (88)$$

**Interfacial entropy inequality and kinetic relations.** In order to obtain the interfacial entropy inequality for the complete mechanical description we have to substitute in (22)  $\sigma^{ij} = -p\delta^{ij} + \sigma^{<ij>}$  instead of  $\sigma^{ij} = -p\delta^{ij}$ . After some simple algebraic manipulations we now end up with

$$\dot{\mathcal{N}}_{\text{Li}}\left[\left[\mu_{\text{Li}} - \mu_{\text{V}} - \frac{m_{\text{Li}}}{\rho}\sigma^{<ij>}\nu^i\nu^j + \frac{m_{\text{Li}}}{2}(v-w)^2\right]\right] + \dot{\mathcal{N}}_{\text{M}}\left[\left[\mu_{\text{V}} - \frac{m_{\text{M}}}{\rho}\sigma^{<ij>}\nu^i\nu^j + \frac{m_{\text{M}}}{2}(v-w)^2\right]\right] \geq 0. \quad (89)$$

The normal  $\nu$ , with  $\nu^i\nu^i = 1$ , of the interface points into the + region. The velocity of the interface is  $w$ , and  $w^\nu$  denotes its normal speed.

We observe that we may read off from (89) kinetic relations of the same formal structure as it is given by (25). The important difference to the case with pure pressure is the contribution of the jump of the stress deviator to the driving forces. Preliminary numerical calculations reveal that this contribution may induce that a spherical as well as a flat interface may become unstable.

**Decomposition of total strain into elastic and misfit strain.** This paragraph introduces the appearing peculiarities that we meet if we describe the deformation of a solid that consists of several constituents. The following discussion gives the basic prerequisite to formulate the appropriate constitutive law that relates the stress to the strain. We choose as variables the Li fraction and the deformation gradient, i.e.  $(y, F)$ .

We consider a reference state  $\bar{S}$  with  $(\bar{y} = 0, \bar{F}^{ij} = \delta^{ij})$ , an intermediate state  $S_*$  with  $(y_* = y, F_*^{ij})$  and the actual state  $S$  with  $(y, F^{ij})$ . We assume, that these states are related to each other by the following conditions: (i) The intermediate state is reached from the reference state under constant reference stress  $\sigma^{ij} = -\bar{p}\delta^{ij}$ . (ii) The transition of the intermediate state to the actual state by  $F_e^{ij}$  at constant Li fraction  $y$  leads to elastic stress  $\sigma^{ij} \neq -\bar{p}\delta^{ij}$ . For this reason we call  $F_e^{ij}$  the elastic part of the deformation gradient.

By means of the given rules we have decomposed the change of the state of a solid into two parts, without and with deviations from the hydrostatic reference stress. The deformation gradient  $F_*^{ij}$  might be due to thermal expansion, which we do not consider here, or/and due to the change of shape and volume because we have a change of the Li fraction from  $\bar{y} = 0$  to  $y_* = y$ . In any case,  $F_*^{ij}$  is experimentally measured at the reference stress. On the other hand, elastic stresses are exclusively due to changes of the atomic distances of the crystal lattice at fixed occupation of lattice sites.

The reference, the intermediate and the actual state have mass densities  $\bar{\rho}$ ,  $\rho_*$ ,  $\rho$ , particle densities  $\bar{n}_{\text{M}}$ ,  $n_{\text{M}}^*$ ,  $n_{\text{M}}$  and Li fractions  $\bar{y} = 0$ ,  $y_* = y$ ,  $y$ . We thus have

$$\bar{\rho} = m(\bar{y})\bar{n}_{\text{M}}, \quad \rho_* = m(y)n_{\text{M}}^*, \quad \text{and} \quad \rho = m(y)n_{\text{M}}, \quad (90)$$

so that the three Jacobians  $J_* = \det(F_*) = \bar{\rho}/\rho_*$ ,  $J_e = \det(F_e) = \rho_*/\rho$  and  $J = \det(F) = \bar{\rho}/\rho$  are given by

$$J_* = \nu(y)\frac{\bar{n}_{\text{M}}}{n_{\text{M}}^*}, \quad J_e = \frac{n_{\text{M}}^*}{n_{\text{M}}}, \quad J = \nu(y)\frac{\bar{n}_{\text{M}}}{n_{\text{M}}} \quad \text{with} \quad \nu \equiv \frac{m(\bar{y})}{m(y)}. \quad (91)$$

There is a multiplicative decomposition of the total deformation gradient according to

$$F^{ij} = F_e^{ik} F_*^{kj}, \quad (92)$$

which results by a simple geometric reasoning: We have three motions: The total motion from  $\bar{S}$  to  $S$ :  $x^i = \chi^i(t, X)$ , the motion at constant reference stress from  $\bar{S}$  to  $S_*$ :  $X_*^i = \chi_*^i(t, X)$  and the pure elastic motion from  $S_*$  to  $S$ :  $x^i = \chi_e^i(t, X_*)$ . The chain rule implies

$$F^{ij} = \frac{\partial \chi^i}{\partial X^j} = \frac{\partial \chi_e^i}{\partial X_*^k} \frac{\partial \chi_*^k}{\partial X^j} = F_e^{ik} F_*^{kj}. \quad (93)$$

**The St. Venant-Kirchhoff law.** We denote the 2<sup>nd</sup> Piola-Kirchhoff stresses with respect to the states  $\bar{S}$  and  $S_*$  by  $t^{ij}$  and  $z^{ij}$ , respectively. Obviously the both stresses give the same (actual) Cauchy stress by

$$\sigma^{ij} = \frac{1}{J} F^{ik} F^{jl} t^{kl} \quad \text{and} \quad \sigma^{ij} = \frac{1}{J_e} F_e^{ik} F_e^{jl} z^{kl}, \quad (94)$$

and by elimination of  $\sigma^{kl}$  we obtain with (92)

$$t^{ij} = J_* F_*^{-ik} F_*^{-jl} z^{kl}. \quad (95)$$

Recall that the transformation from  $S_*$  to  $S$  is purely elastic, so that we have to formulate the elastic stress strain relation for  $z^{ij}$ . For small strains we may use the St. Venant-Kirchhoff law which reads

$$z^{ij} = -\bar{p} J_e C_e^{-ij} + \frac{1}{2} \tilde{K}^{ijkl}(y) (C_e^{kl} - \delta^{kl}). \quad (96)$$

$C_e^{ij} = F_e^{ki} F_e^{kj}$  is the elastic Cauchy-Green tensor. The stiffness matrix  $\tilde{K}^{ijkl}(y)$  depends on the Li fraction and satisfies the general symmetries  $\tilde{K}^{ijkl} = \tilde{K}^{jikl} = \tilde{K}^{ijlk} = \tilde{K}^{klij}$ .

In order to obtain the free energy density according to (88) we have to calculate the stress-strain relation for the stress  $t^{ij}$ . We insert the elastic law (96) into (95) and define a stiffness matrix  $K^{ijkl}$  and a misfit strain  $C_*^{ij}$  by

$$K^{ijkl}(y) \equiv J_* F_*^{-im} F_*^{-jn} F_*^{-ko} F_*^{-lp} \tilde{K}^{mnop}(y) \quad \text{and} \quad C_*^{ij} \equiv F_*^{ki} F_*^{kj}. \quad (97)$$

After some algebraic manipulations we finally obtain

$$t^{ij} = -\bar{p} J C_*^{-ij} + \frac{1}{2} K^{ijkl}(y) (C^{kl} - C_*^{kl}(y)). \quad (98)$$

The experimental data given by Maxisch and Ceder, [9] can be used to calculate the various components of the stiffness matrix and the misfit strain. Unfortunately the authors do not indicate whether their measurements rely on the stress-strain relation (96) or on (98). However, we think they have used (96).

**Free energy density and chemical potentials for the St.Venant-Kirchhoff law.** The mechanical part of the free energy density relies on the thermodynamic relation (88). By simple integration and by including the chemical part we obtain

$$\rho\psi = n_M\Omega f(y) + \bar{p}\left(\frac{J_*}{J} - 1\right) + \frac{1}{8J}(C^{kl} - C_*^{kl})K^{klmn}(C^{mn} - C_*^{mn}). \quad (99)$$

In order to calculate the chemical potentials according to (87)<sub>1,2</sub>, we must represent  $\rho\psi$  in the variables  $n_{\text{Li}}$ ,  $n_V$  and  $c^{ij}$ , recall  $c^{ij} = (\nu(y)\bar{n}_M/n_M)^{-2/3}C^{ij}$ . We obtain for lithium

$$\begin{aligned} \mu_{\text{Li}} = & \Omega(f + (1 - y)f') + \\ & \frac{1}{\bar{n}_M\nu}\left(\left(\frac{m_{\text{Li}}}{m_M}\nu(1 - y) + 1\right)(\bar{p}J_* - \frac{1}{8}\left(\frac{1}{3}C^{kl} + C_*^{kl}\right)K^{klmn}(C^{mn} - C_*^{mn})) + \right. \\ & \left. (1 - y)(\bar{p}J'_* + \frac{1}{8}(C^{kl} - C_*^{kl})K'^{klmn}(C^{mn} - C_*^{mn}) - \frac{1}{2}C_*'^{kl}K^{klmn}(C^{mn} - C_*^{mn}))), \end{aligned} \quad (100)$$

and for the vacancies

$$\begin{aligned} \mu_V = & \Omega(f - yf') + \\ & \frac{1}{\bar{n}_M\nu}\left(-\left(\frac{m_{\text{Li}}}{m_M}\nu y - 1\right)(\bar{p}J_* - \frac{1}{8}\left(\frac{1}{3}C^{kl} + C_*^{kl}\right)K^{klmn}(C^{mn} - C_*^{mn})) - \right. \\ & \left. y(\bar{p}J'_* + \frac{1}{8}(C^{kl} - C_*^{kl})K'^{klmn}(C^{mn} - C_*^{mn}) - \frac{1}{2}C_*'^{kl}K^{klmn}(C^{mn} - C_*^{mn}))), \end{aligned} \quad (101)$$

where a prime indicates the derivative with respect to the Li fraction  $y$ .

Thus we have completed the constitutive theory for the host system with chemical and mechanical coupling.

## References

- [1] J.L. Allen, T.R. Jow and J. Wolfenstine, *Kinetic Study of the Electrochemical FePO<sub>4</sub> to LiFePO<sub>4</sub> Phase transition*, Chemical Materials **19** (2004), 2108–2111.
- [2] T. Böhme, W. Dreyer, F. Duderstadt, and W.H. Müller *A higher gradient theory of mixtures for multi-component materials*, WIAS Preprint No. 1286, Philosophical Magazine submitted (2007).
- [3] W. Dreyer, *Jump Conditions at phase boundaries for ordered and disordered phases*, WIAS Preprint No. 869 (2003).
- [4] W. Dreyer and F. Duderstadt, *On the modelling of semi-insulating GaAs including surface tension and bulk stresses*, WIAS Preprint No. 995, to appear in Proc. R. Soc. A (2008).

- [5] M. Gaberšček, R. Dominko and J. Jamnik, *The meaning of impedance measurements of  $\text{LiFePO}_4$  cathodes: A linearity study*, J. power sources **174** (2007), 944-948.
- [6] M. Gaberšček, R. Dominko, M. Bele, M. Remškar, D. Hanzel and J. Jamnik, *Porous, carbon-decorated  $\text{LiFePO}_4$  prepared by sol-gel method based on citric acid*, Solid State Ionics **176** (2005), 1801–1805.
- [7] P.M. Gomadam and J.W. Weidner, *Modeling Volume Changes in Porous Electrodes*, Journal of The Electrochemical Society **153**(1) (2006), A179–A186.
- [8] B.C. Han, A. Van der Ven, D. Morgan and G. Ceder, *Electrochemical modeling of intercalation processes with phase field models*, Electrochimica Acta **49** (2004), 4691–4699.
- [9] T. Maxisch and G. Ceder, *Elastic properties of olivine  $\text{Li}_x\text{FePO}_4$  from first principles*, Physical Review B **73** (2006), 174112-1–174112-4.
- [10] V. Srinivasan and J. Newman, *Discharge Model for the Lithium Iron-Phosphate Electrode*, Journal of The Electrochemical Society **151**(10) (2004), A1517–A1529.
- [11] M. Wagemaker, W.J.H. Borghols and F.M. Mulder, *Large Impact of Particle Size on Insertion Reaction. A Case for Anatase  $\text{Li}_x\text{TiO}_2$* , J. AM. CHEM. SOC. **129**(14) (2007), 4323–4327.
- [12] A. Yamada, H. Koizumi, S.I. Nishimura, N. Sonoyama, R. Kanno, M. Yone-mura, T. Nakamura and Y. Kobayashi, *Room-temperature miscibility gap in  $\text{Li}_x\text{FePO}_4$* , Nature materials Letters **5** (2006), 357–360.